

See discussions, stats, and author profiles for this publication at: <https://www.researchgate.net/publication/231672494>

Investigation of Structures in Polyelectrolyte/Surfactant Complexes by X-ray Scattering

ARTICLE *in* LANGMUIR · MAY 2001

Impact Factor: 4.46 · DOI: 10.1021/la001249x

CITATIONS

52

READS

23

5 AUTHORS, INCLUDING:



[Ksenija Kogej](#)

University of Ljubljana

62 PUBLICATIONS 880 CITATIONS

SEE PROFILE



[H. Reynaers](#)

University of Leuven

29 PUBLICATIONS 685 CITATIONS

SEE PROFILE

Investigation of Structures in Polyelectrolyte/Surfactant Complexes by X-ray Scattering

Ksenija Kogej,^{*,†,‡} Guennady Evmenenko,[†] Elisabeth Theunissen,[†]
Hugo Berghmans,[†] and Harry Reynaers[†]

Department of Chemistry, Catholic University of Leuven, Celestijnenlaan 200F,
B-3001 Heverlee, Belgium, and Faculty of Chemistry and Chemical Technology, University of
Ljubljana, Aškerčeva 5, P.O.B. 537, SI-1001 Ljubljana, Slovenia

Received August 30, 2000. In Final Form: November 28, 2000

Structural investigation in systems of anionic polyelectrolytes and dodecyl- (DPC) and cetylpyridinium chlorides (CPC) were performed at various surfactant to polyelectrolyte (S/P) ratios using synchrotron X-ray scattering. The polyelectrolytes used were sodium poly(styrenesulfonate) (NaPSS), poly(acrylate) (NaPA), and poly(methacrylate) (NaPMA). From the Bragg peaks emerging in the scattering curves, different types of organization of the surfactant in conjunction with the polyion are proposed. They depend on the surfactant chain length, on the polyelectrolyte chemistry, and on the S/P value: (1) NaPSS/DPC (all S/P values), NaPSS/CPC (S/P < 1), and NaPA(NaPMA)/DPC (S/P < 1) complexes produced a micellelike organization of the surfactant along the polyion chain. The NaPSS-induced micelle is smaller in size than the ordinary one because of the inclusion of the aromatic rings on the PSS chain into the hydrophobic interior of the micelle. The size of the ordered elements in complexes with the hydrophilic NaPA and NaPMA corresponds to the radius of an ordinary globular micelle together with the thickness of the polyelectrolyte chain that surrounds it. (2) In NaPSS/CPC precipitate (S/P ≥ 1), a hexagonal phase is observed with a unit cell parameter equal to 39.5 Å. (3) The multiple reflections in the scattering curves of NaPA(NaPMA)/DPC complexes with S/P ≥ 1 and of NaPA(NaPMA)/CPC ones for all S/P values point to some cubic structure. The cell constants of these mesophases correspond approximately to 2.5 diameters of a globular surfactant micelle. (4) In addition to a cubic phase, a well-pronounced hexagonal phase with a unit cell parameter of 40.5 Å develops in the NaPA/CPC case with S/P ≥ 1.

Introduction

Ionic surfactants form complexes with oppositely charged polyelectrolytes already in extremely dilute aqueous solutions.¹ In these complexes, the surfactant is aggregated into the so-called polyion-induced micelles which behave as multivalent counterions and become trapped in the regions of high electrostatic field around the macroion. The predominant attractive force between the charged polymer chain and the micellized surfactant is therefore electrostatic and is governed by the charge density of the chain and of the surfactant micelle.

Additional important differences between various polyelectrolyte–surfactant systems originate from the specific properties of the macroion chain, for example, from its flexibility and in particular from its hydrophilic/hydrophobic character. Functional groups of the repeating unit on the polyion are often aromatic rings that can solubilize inside the surfactant micelle.^{2,3} A typical example is the chain of the polystyrenesulfonate anion with benzene-

sulfonate functional groups attached to its backbone. In this case, in comparison with purely hydrophilic chains that display chiefly electrostatic interactions with surfactant, very stable aggregates are formed by inclusion of the aromatic ring into the hydrophobic interior of the micelle. One can visualize these aggregates as mixed micelles, particularly because they show properties of individual, though rather complex, ionic species in solution.⁴ Another important class of polymers are the hydrophobically modified ones.⁵ It is convenient to group polyelectrolyte–surfactant complexes in the order of increasing hydrophobic character of the polyion^{1b,8} into those containing (1) hydrophilic polyelectrolytes, (2) hydrophobic polyelectrolytes, or (3) hydrophobically modified ones. In this paper, we shall confine ourselves to the investigation of the first two groups and their typical representatives, that is, poly(acrylate), PA, poly(methacrylate), PMA, and poly(styrenesulfonate), PSS, chains.

Previous studies of surfactant binding to polyion chains that have the same charge density but different hydrophobic character,^{6–8} for example, to PA and PSS anions, point to some subtle differences in their interactions with cationic alkylpyridinium surfactants. The binding starts at lower free surfactant concentrations and continues to almost quantitative association (100% binding)⁸ in the

* Corresponding author: Ksenija Kogej, Department of Chemistry, Catholic University of Leuven, Celestijnenlaan 200F, B-3001, Leuven-Heverlee, Belgium. Fax: +32-16-32-7990. E-mail: ksenija.kogej@chem.kuleuven.ac.be.

† Catholic University of Leuven.

‡ University of Ljubljana.

(1) (a) *Polymer-Surfactant Systems*; Surfactant Science Series; Kwak, J. C. T., Ed.; Marcel Dekker: New York, 1998; Vol. 77. (b) Linse, P.; Picelle, L.; Hansson, P. In *Polymer-Surfactant Systems*; Surfactant Science Series; Kwak, J. C. T., Ed.; Marcel Dekker: New York, 1998; pp 193–238. (c) Ananthapadmanabahn, K. P. In *Interactions of Surfactants with Polymers and Proteins*; Goddard, E. D., Ananthapadmanabahn, K. P., Eds.; CPC Press: Boca Raton, FL, 1993; pp 319–365.

(2) Gao, Z.; Wasylishen, R. E.; Kwak, J. C. T. *J. Colloid Interface Sci.* **1988**, *126*, 371.

(3) Kogej, K.; Škerjanc, J. *Langmuir* **1999**, *15*, 4251.

(4) Škerjanc, J.; Kogej, K. In *Macroion Characterization. From Dilute Solutions to Complex Fluids*; Schmitz, K. S., Ed.; ACS Symposium Series; American Chemical Society: Washington, DC, 1994; Chapter 20, p 268.

(5) *Macromolecular Complexes in Chemistry and Physics*; Dubin, P., Bock, J., Shulz, D. N., Thies, C., Eds.; Springer-Verlag: Berlin-Heidelberg, 1994.

(6) Kogej, K.; Škerjanc, J. *Acta Chim. Slov.* **1998**, *45*, 443.

(7) Kogej, K.; Škerjanc, J. *Acta Chim. Slov.* **1999**, *46* (2), 269.

(8) Kogej, K.; Škerjanc, J. In *Physical Chemistry of Polyelectrolytes*; Surfactant Science Series; Radeva, Ts., Ed.; Marcel Dekker: New York, 2001; Vol. 99, Chapter 21, pp 793–827.

case of a slightly hydrophobic PSS chain, whereas with the hydrophilic PA anion the onset of surfactant fixation to the polyion is shifted to higher free surfactant concentrations.^{6–8} The saturation of the PA chain is achieved already when less than an equivalent amount of surfactant has been added to the solution. Simultaneously, in the presence of PA the precipitation caused by the addition of surfactant to the polyelectrolyte takes place at lower surfactant to polyelectrolyte charge ratios than in the PSS solutions. Visually, the precipitates are very different: the complex of surfactant with PA is a sticky phase whereas the one with PSS is a powderlike precipitate. The precipitate with PSS is readily redissolved by adding a small amount of excess surfactant (or polyelectrolyte),⁴ whereas with PA this does not happen so easily.

Most of the knowledge concerning the phase behavior of polyelectrolyte–surfactant systems comes from the systematic study conducted by Thalberg et al.,¹⁰ these investigations involve hyaluronate and PA anion and a series of alkyltrimethylammonium cations. To our knowledge, only one study of phase behavior including the PSS anion is reported.¹¹ That investigation involves dodecyltrimethylammonium bromide, DTAB, as the oppositely charged surfactant. It was concluded therein¹¹ that the phase behavior in the PSS/DTAB system differs from what was found in other systems.¹⁰ One can conclude from the above considerations that the nature of the chain has a strong influence on the phase behavior in polyelectrolyte–surfactant mixed systems. It is likely that this is reflected also in the precise structure of the polyelectrolyte–surfactant complex.

It has been known already for some time that the precipitates or highly dense phases that result from the complexation of surfactant with the polyelectrolyte can be ordered. Carnali¹² found a hexagonal phase in the phase diagram of 50% neutralized sodium poly(acrylate), NaPA, tetradecyltrimethylammonium bromide, and water. Likewise, Ilekli et al.¹³ found cubic, hexagonal, and lamellar phases in a phase diagram of stoichiometric complexes between NaPA and cetyltrimethylammonium bromide. Ordered structures have been observed also in systems of covalently cross-linked polyelectrolyte gels, either in a lamellar,¹⁴ cubic,^{15,16} or hexagonal arrangement.^{17,18}

In the work reported here, our purpose is to obtain information about the structural properties of complexes formed between NaPA, NaPMA, and NaPSS and alkylpyridinium salts with two different lengths of the hydrocarbon chain, that is, dodecylpyridinium and cetylpyridinium chloride. The structural properties of complexes will be examined by means of synchrotron X-ray scattering (SAXS) in a wide range of surfactant to polyelectrolyte ratios. These systems were thoroughly studied in the dilute regime, typically at a polyelectrolyte concentration around 5×10^{-4} monomol/L and mostly below an equimolar

surfactant to polyelectrolyte ratio.^{6–9,19–22} Our investigation is extended to higher polymer concentrations, in the order of 1% (50–100 times higher than stated above), and includes also 1:1 and higher molar ratios between the surfactant and polyion charges.

Experimental Section

Materials. Sodium poly(styrenesulfonate) (NaPSS) with a molar mass of about 70 kg/mol and a degree of sulfonation of 1.0, supplied by Polysciences, Inc. (Warrington, PA), was prepared and purified by the procedure described in the literature.⁹ Poly(acrylic acid) with a molar mass of about 10 kg/mol was supplied from K&K Laboratories, Inc., Plainview, NY. The procedure for the purification was reported previously.^{23–24} From the acid, the sodium salt (NaPA) was prepared by neutralization with NaOH. Poly(methacrylic acid) (PMA) was synthesized from methacrylic acid by radical polymerization. The weight average molar mass of PMA was determined by wide-angle laser light scattering. The value of 180 kg/mol was found. Sodium poly(methacrylate) (NaPMA) was obtained by neutralization of the acid. The pH of the NaPMA stock solution was around 9.5. The surfactants, *N*-cetylpyridinium chloride (CPC, puriss, Kemika Zagreb, Croatia) and *N*-dodecylpyridinium chloride (DPC, a gift from Merck-Schuchardt), were repeatedly recrystallized from acetone and dried under vacuum at 50 °C. All solutions were prepared with ultrapure water obtained from a Milli-Q-Reagent Grade Water System, Millipore. The specific conductance of water was below $1 \times 10^{-6} \Omega^{-1} \text{ cm}^{-1}$.

Preparation of Samples. In the first place, aqueous solutions of polyelectrolytes were prepared from stock solutions of known concentration. An aqueous medium without addition of simple salt was chosen in order to study the situation of the strongest binding of DP⁺ and CP⁺ cations to these polyanions.^{6–9,19} The polyelectrolyte concentration in the final mixed solutions with surfactants was 0.05 monomol/L expressed in moles of monomer units per volume. This corresponds to 0.47, 0.54, and 1.0 vol % for NaPA, NaPMA, and NaPSS, respectively. Pure DPC and CPC solutions above their critical micellization concentration (cmc) in water were used for the preparation of mixed solutions with polyions. The mixed polyelectrolyte–surfactant complex solutions were prepared by slowly adding the appropriate amount of DPC or CPC stock solutions in water to the polyelectrolyte solution at room temperature under stirring. All mixed solutions were studied in a wide range of surfactant to polyelectrolyte molar ratios, denoted by S/P, from 0 up to 1.5. The measurements in polyelectrolyte–surfactant complex solutions were performed at 25 °C. Scattering from pure DPC and CPC solutions above cmc, that is, in 1, 5, and 10 vol % aqueous solution without simple salt, was detected in order to determine the surfactant aggregation number at 25 °C. A 20 vol % CPC solution was used for temperature studies. This concentration is already above the saturation point at room temperature. The clear supersaturated solution can be prepared by gently warming a 20% solution up to about 30 °C. It remains in this metastable state for some time even after cooling it to 25 °C. This solution was then used to fill a thermostated sample holder and was cooled with a rate of 1 °C/min in the range from 25 to 10 °C.

Visual Appearance of Samples. After the addition of DPC or CPC to NaPA and NaPMA solutions, instantaneously an inhomogeneous but stable white colloidal solution was formed. The turbidity of the solution was less pronounced in the DPC than in the CPC case and increased for both surfactants with the increasing the S/P ratio; however, no precipitate separated from the solutions for S/P ≤ 0.7. At S/P ratios close to or higher than one, sticky pieces of polyelectrolyte–surfactant complex formed in a still turbid solution. Both the sticky precipitate and the equilibrium solution were analyzed by SAXS.

Mixed NaPSS/DPC and NaPSS/CPC solutions are completely transparent up to S/P ratios a little above 0.7.^{4,11,19} At higher surfactant content, the solutions become turbid and at

(9) Škerjanc, J.; Kogej, K.; Vesnaver, G. *J. Phys. Chem.* **1988**, *92*, 6382.

(10) (a) Thalberg, K.; Lindman, B. *J. Phys. Chem.* **1990**, *94*, 4289. (b) Thalberg, K.; Lindman, B.; Bergfeldt, K. *Langmuir* **1991**, *7*, 2893.

(11) Hansson, P.; Almgren, M. *Langmuir* **1994**, *10*, 2115.

(12) Carnali, J. O. *Langmuir* **1993**, *9*, 2933.

(13) (a) Ilekli, P.; Piculell, L.; Tournilhac, F.; Cabane, B. *J. Phys. Chem. B* **1998**, *102*, 344. (b) Ilekli, P.; Martin, T.; Cabane, B.; Piculell, L. *J. Phys. Chem. B* **1999**, *103*, 9831.

(14) Mironov, A. V.; Starodoubtsev, S. G.; Khokhlov, A. R.; Dembo, A. T.; Yakunin, A. N. *Macromolecules* **1998**, *31*, 7698.

(15) Hansson, P. *Langmuir* **1998**, *14*, 4059.

(16) Okuzaki, H.; Osada, Y. *Macromolecules* **1995**, *28*, 380.

(17) Chu, B.; Yeh, F.; Sokolov, E. L.; Starodoubtsev, S. G.; Khokhlov, A. R. *Macromolecules* **1995**, *28*, 8447.

(18) Dembo, A. T.; Yakunin, A. N.; Zaitsev, V. S.; Mironov, A. V.; Starodoubtsev, S. G.; Khokhlov, A. R.; Chu, B. *J. Polym. Sci. Phys.* **1998**, *34*, 2893.

(19) Škerjanc, J.; Kogej, K. *J. Phys. Chem.* **1989**, *93*, 7913.

(20) Hayakawa, K.; Kwak, J. C. T. *J. Phys. Chem.* **1982**, *86*, 3866.

(21) Hayakawa, K.; Kwak, J. C. T. *J. Phys. Chem.* **1983**, *87*, 506.

(22) Abiun, E. B.; Scaiano, J. C. *J. Am. Chem. Soc.* **1984**, *106*, 6274.

approximately a 1:1 charge ratio a white complex phase-separates from the solution. The PSS[−]/DP⁺ complex is a slightly sticky phase, whereas the PSS[−]/CP⁺ one is a powderlike white precipitate. The equilibrium solution is a transparent waterlike phase. It contains a rather low amount of excess surfactant and NaCl. The latter one results from the complexation reaction between the polyelectrolyte and surfactant.^{3,14}

Synchrotron X-ray Measurements. Small-angle X-ray experiments were performed on SAXS/WAXS beam line BM26 (DUBBLE) at the European Synchrotron Radiation Facility (ESRF, Grenoble).²⁵ The monochromatic incident light from the radiation spectrum of the source was obtained by using a double-crystal Si(111) monochromator with sagittal focusing on the second crystal to give an intense monochromatic X-ray beam in the range from 5 to 30 keV. The beam had a fixed exit height and a transmission bandwidth of $\Delta\lambda/\lambda \approx 2 \times 10^{-3}$. The optical bench allowed variation of the sample-to-detector distance from 1.0 to 7.0 m, covering the scattering vector $|\mathbf{q}|$ ($= q = (4\pi/\lambda) \sin \theta$, where λ is the wavelength and 2θ is the scattering angle) in the range from 0.01 to 0.5 Å^{−1}. The beam line is equipped with a two-dimensional gas-filled wire-chamber SAXS detector. Silver behenate was used as a low-angle and rat-tail as a high-angle diffraction standard to check the proper alignment and to calibrate the instrumentation.²⁶ The SAXS data were normalized to the intensity of the primary beam and corrected for the detector response. The background scattering due to the solvent was subtracted from the scattering curves by taking into account the differences in the absorption of the solution and the solvent. For the preliminary treatment of data, the software packages BSL²⁷ and FIT2D²⁸ were used. The samples for measurements were filled in a thermally isolated sample holder. For isothermal measurements, the temperature was kept at 25 °C with a precision and temperature stability better than 0.1 °C.

General Remarks on Scattering Curves from Surfactant–Polyelectrolyte Solution. The small-angle X-ray scattering technique is an important tool that is often employed to obtain information on the size and structure of condensed matter. The appearance of diffraction peaks in the SAXS profiles is an indication of a high degree of order in the system. The most highly ordered form of association of atoms or molecules is a crystal. Powder or diffraction patterns of crystalline structures are composed of sharp lines (Bragg peaks) from which the lattice type of a substance and the lattice constant can be determined.

Two types of disorder may coexist in a real “ordered” system.²⁹ Thermal motion causes the atoms to deviate from their ideal positions. In this case, the long-range order (periodicity) is retained and all peaks in the distribution function have the same shape no matter what their distance from the zero-order peak. Characteristic for liquids and assemblies of chain molecules, not possessing strict periodicity, are the distortions of the second kind. In this case, only the short-range order is retained, as there are no fixed equilibrium positions throughout the sample. However, one can always state the mean distance between the first neighbors from the position of the peak in the scattering curve.

Scherrer³⁰ showed that the mean crystallite size in a given sample is related to the pure X-ray diffraction line broadening and may be estimated from Bragg peaks by the equation

$$L = \frac{\lambda}{\beta_S \cos \theta} \quad (1)$$

where β_S is the full width at a half-maximum intensity of the peak observed at a mean scattering angle of 2θ and λ is the wavelength of the incident beam. The value of β_S is obtained by

(23) Škerjanc, J.; Pavlin, M. *J. Phys. Chem.* **1977**, *81*, 1166.

(24) Škerjanc, J. *Biophys. Chem.* **1974**, *1*, 376.

(25) Bras, W. *J. Macromol. Sci., Phys.* **1998**, *B37* (4), 557.

(26) Huang, T. C.; Toraya, H.; Blaton, T. N.; Wu, Y. *J. Appl. Crystallogr.* **1993**, *26*, 180.

(27) Mant, G. R. Daresbury Laboratory. Private communication.

(28) Hammersley, A. ESRF, Grenoble. Private communication.

(29) Vainshtein, B. K. *Diffraction of X-rays by Chain Molecules*; Elsevier: Amsterdam-London-New York, 1996; Chapter 5, pp 203–254.

(30) Scherrer, P. *Göttinger Nachrichten* **1918**, *2*, 98.

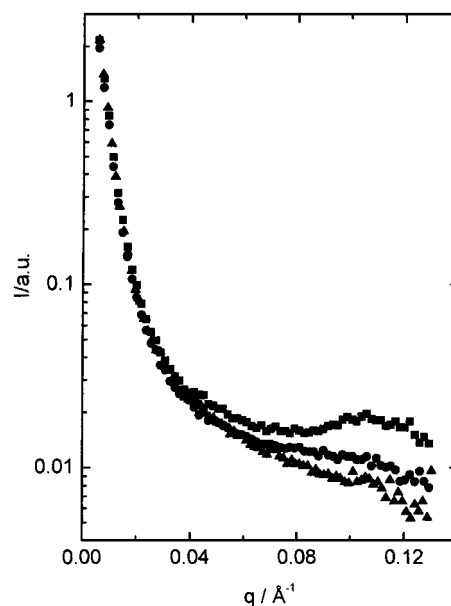


Figure 1. SAXS patterns for different concentrations of DPC in water at 25 °C: (▲) 1%, (●) 5%, and (■) 10%.

modeling the Bragg peak in SAXS curves using a Gaussian function. Parameter L is a measure of the mean long-range order in the system. Moreover, an “interaction radius” (r_m) of scattering entities and a degree of disorder (Δ/\bar{a}) in the system can be obtained from expressions 2 and 3:²⁹

$$r_m = \left(\frac{\pi}{2.5} \right)^2 \frac{\lambda}{\beta_S} \quad (2)$$

$$\Delta/\bar{a} = \frac{1}{\pi} \sqrt{\frac{\beta_S \bar{a}}{\lambda}} \quad (3)$$

The region outside which the distribution function becomes practically smooth and approaches the mean value defines the interaction radius (r_m). In eq 3, Δ is the width of fluctuations in distances between the neighboring scattering units and \bar{a} ($= 2\pi/q_m$, where q_m is the value of the scattering vector corresponding to the peak maximum) is the characteristic size of the ordered elements. In the case of a pure surfactant solution above the cmc, \bar{a} ($\equiv d$) corresponds to the most probable intermicellar distance. “Gas”-type scattering with no maximum in the scattering curve occurs if the degree of disorder Δ/\bar{a} exceeds 0.25–0.3, whereas for $\Delta/\bar{a} \approx 0.2$ one already observes a strong first maximum. Formally speaking, reduction in Δ/\bar{a} would bring us to the crystalline lattice; however, only high values of this parameter are characteristic for real objects.²⁹

Results and Structural Analysis

First, the treatment of scattering curves obtained from pure surfactant solutions above their cmc at 25 °C and during cooling from 25 to 10 °C is presented. Afterward, the isothermal measurements in polyelectrolyte–surfactant mixtures at a fixed polyelectrolyte concentration and increasing S/P ratio are discussed. Measurements in pure surfactant solutions are included to demonstrate the differences in surfactant self-association in the absence and in the presence of the polyelectrolyte. By no means was the purpose of these experiments to give a full account on structures or phase behavior in CPC (or DPC)/water systems.

I. Pure Surfactant Solutions. 1. DPC and CPC Solutions at 25 °C. Figures 1 and 2 show the scattering patterns obtained in pure 1, 5, and 10 vol % DPC and CPC solutions, respectively. These concentrations are well above the cmc values of these two surfactants in water at

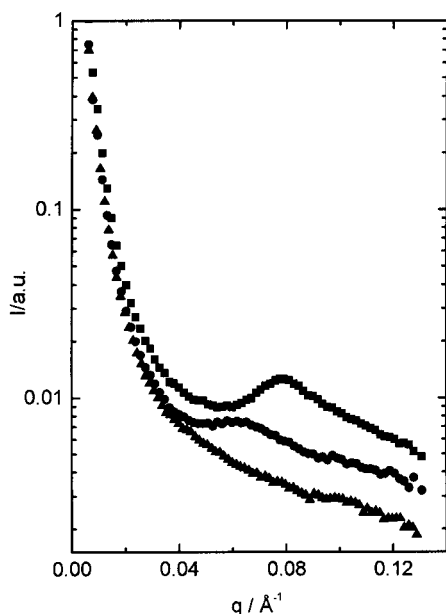


Figure 2. SAXS patterns for different concentrations of CPC in water at 25 °C: (▲) 1%, (●) 5%, and (■) 10%.

25 °C, which are 1.52×10^{-2} mol/L (or 0.43 vol %) and 6.3×10^{-4} mol/L (or 0.02 vol %) for DPC and CPC, respectively.⁹ One can see that a scattering peak occurs for sufficiently high surfactant concentrations (in 10% DPC and CPC solutions, whereas in 5% CPC it is less pronounced) at the q_m -value corresponding to the most probable intermicellar distance $d (= 2\pi/q_m)$. Evidently, the peak position moves to higher q -values (shorter intermicellar distances) with increasing surfactant concentration. The q_m -values are 0.107 and 0.081 Å⁻¹ for 10% DPC and CPC solutions, respectively, and the corresponding center-to-center separation of micelles is 58.6 and 77.5 Å. Taking into account the total amount of surfactant present in the solution, the aggregation numbers of DPC and CPC in water can be calculated from these distances. They are 42 and 77 for DPC and CPC, respectively. These values are in reasonable agreement with the literature experimental data^{31,32} and with estimations of aggregation numbers based on the apparent molar volume measurements for alkylpyridinium bromides.³³

2. 20% CPC Solution: Cooling in the Range from 25 to 10 °C. SAXS patterns of a 20% CPC solution, obtained during cooling from 25 to 10 °C with a rate of 1 °C/min and subsequently staying at 10 °C, are shown in Figure 3. During this process, the CPC solution completely transforms into a solid. It has to be pointed out that these are dynamic measurements. Only curves 1 and 4 correspond to an equilibrium state. One can clearly see the buildup of the order in the system. The diffraction patterns in curves 1 and 2 show only one structure factor peak; its position corresponds to a mean distance between CPC micelles at this surfactant concentration. In curve 3, one detects three peaks, and finally in curve 4 four peaks are seen. The analysis of curve 3 reveals that the positions of the three peaks are at q_m -values equal to 0.0969, 0.2004, and 0.3971 Å⁻¹, or the distances d are equal to 64.8, 31.4, and 15.8 Å. The ratios of $q_{m,2}/q_{m,1} (= d_1/d_2)$ and $q_{m,3}/q_{m,2} (= d_2/d_3)$ are both equal to 2. The positions of peaks in

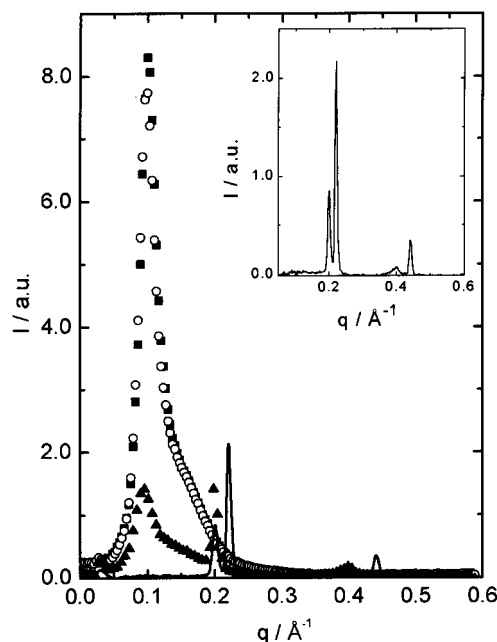


Figure 3. SAXS patterns for a 20% solution of CPC, obtained during cooling in the range from 25 to 10 °C: (■) 25 °C (curve 1), (○ and ▲) some intermediate temperature between 25 °C and 10 °C (curves 2 and 3, respectively), and (solid curve) 10 °C (curve 4). In the inset, the scattering at 10 °C is shown in more detail.

curve 4 (see inset in Figure 3) are at $q_m = 0.201, 0.221, 0.398$, and 0.442 Å⁻¹. The d -spacings are 31.4, 28.4, 15.8, and 14.2 Å, and the corresponding $\sin^2 \theta$ values for each diffraction peak fit the sequence 5:6 and for the higher order reflections 20:24. At the moment, we are not able to evaluate the precise features of these structures. Just for the lowest temperature, one would come to a stable crystalline-type ordering of the CPC micelles. By proposing a cubiclike arrangement⁴¹ of CPC, one would obtain a cell constant around 70 Å.

II. Polyelectrolyte–Surfactant Complex Solutions. A. Solutions with DPC. 1. DPC + NaPSS. The scattering curves obtained in mixed NaPSS/DPC solutions are shown in Figure 4. The curves with S/P = 0.9 and 1.5 correspond to a milky solution of a complex and to the precipitated 1:1 complex, respectively. The scattering pattern of pure NaPSS in water displays a smooth decay over the whole q -range studied, indicating the absence of any intermolecular ordering. After the addition of surfactant to the polyelectrolyte, a broad diffraction maximum emerges in a q -range from about 0.24 to 0.19 Å⁻¹. In the inset of Figure 4, the interference maxima after subtracting the background are shown for S/P = 0.3, 0.5, and 0.7. The maxima for S/P = 0.9 and 1.5 retain their original shape after the correction for the background scattering. The q_m -values and the distances $\bar{a} (= 2\pi/q_m)$ between the neighboring scattering units are reported in Table 1. One can see that the increase in the S/P ratio causes the peak to shift to lower q_m -values. Consequently, the characteristic size of the ordered elements (\bar{a}) increases from 25.8 to 33.1 Å for S/P = 0.3 and 1.5, respectively. According to Tanford,³⁵ the length of an extended dodecyl (C₁₂) chain embedded in a micellar core is 15.42 Å. Therefore, the reported distances in the NaPSS/DPC complex are com-

(31) Fujio, K.; Ikeda, S. *Langmuir* **1991**, 7, 2899.

(32) McGinnis, T.; Woolley, M. E. *J. Chem. Thermodyn.* **1997**, 29, 401.

(33) Škerjanc, J.; Kogej, K.; Cerar, J. *Langmuir* **1999**, 15, 5023.

(34) Klug, H. P.; Alexander, L. E. *X-ray Diffraction Procedures for Polycrystalline and Amorphous Materials*; Wiley: New York, 1974; p 419.

(35) Tanford, C. *The Hydrophobic Effect: Formation of Micelles and Biological Membranes*; Wiley: New York, 1973; p 52.

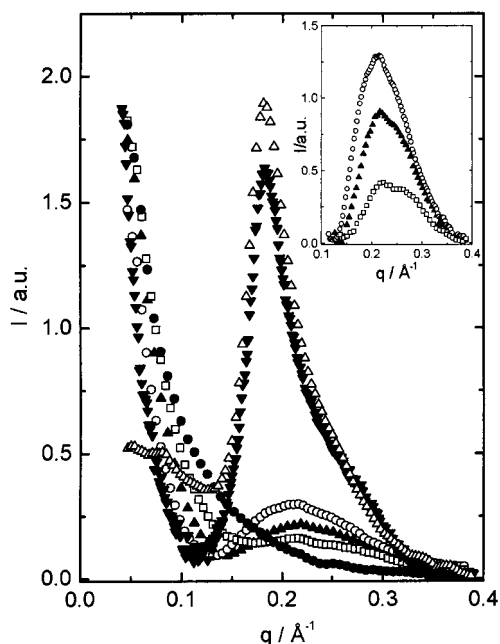


Figure 4. SAXS patterns for pure 1% NaPSS (●) and for NaPSS/DPC complexes with increasing S/P ratios in water: S/P = 0.3 (□), 0.5 (▲), 0.7 (○), 0.9 (△), and 1.5 (▼). In the inset, the scattering in the region of the interference maximum, after subtracting the background, is shown for solutions with S/P = 0.3, 0.5, and 0.7.

Table 1. Structural Parameters of NaPSS/DPC and NaPSS/CPC Complexes in Water Obtained from the Peak(s) in the SAXS Curves

system	S/P	$q_m/\text{\AA}^{-1}$	$\bar{a}/\text{\AA}$	$\beta_s \times 10^2/\text{rad}$	$L/\text{\AA}$	$r_m/\text{\AA}$	Δ/\bar{a}
NaPSS/DPC	0.3	0.243	25.8	2.18	52	82	0.22
	0.5	0.231	27.3	1.76	64	101	0.21
	0.7	0.222	28.4	1.69	67	106	0.21
	0.9	0.193	32.6	1.16	107	170	0.18
	1.5	0.190	33.1	1.02	118	186	0.16
NaPSS/CPC	0.3	0.178	35.2	12.5	90	142	0.20
	0.5	0.173	36.3	12.9	88	138	0.20
	0.7	0.165	38.0	11.2	92	159	0.20
	1.0 (peak 1)	0.157	40.1				
	1.0 (peak 2)	~0.257	24.4				
	1.0 (peak 3)	0.312	20.2				
	1.3 (peak 1)	0.159	39.5				
	1.3 (peak 2)	0.274	22.9				
	1.3 (peak 3)	0.317	19.8				

parable to two hydrocarbon chain lengths. Simultaneously with the decrease of q_m , the intensity of the peaks increases, at first monotonically, but shows a jump at S/P = 0.9. This is an indication that the ordering in the system noticeably increases when the 1:1 charge ratio is approached. All the structural parameters obtained from the curves are collected in Table 1. The mean long-range order L and the interaction radius r_m are relatively constant up to S/P = 0.7. The degree of disorder Δ/\bar{a} is around 0.21. According to Vainshtein,²⁹ this value lies on the boundary between the liquid-type scattering with at least one peak in the scattering curve and gas-type scattering where no peak is observed. The increase in ordering for S/P = 0.9 and 1.5 is indicated by appreciably higher L - and r_m -values and lower Δ/\bar{a} values.

2. DPC + NaPA or NaPMA: $S/P \leq 0.7$. The samples with these S/P values are turbid but not phase-separated. Figures 5 and 6 show scattering patterns for pure NaPA and NaPMA solutions and for NaPA/DPC and NaPMA/DPC complex solutions. Again, a peak emerges in the solutions of the polyelectrolyte-surfactant complex. In comparison with the NaPSS/DPC case, it is shifted to lower

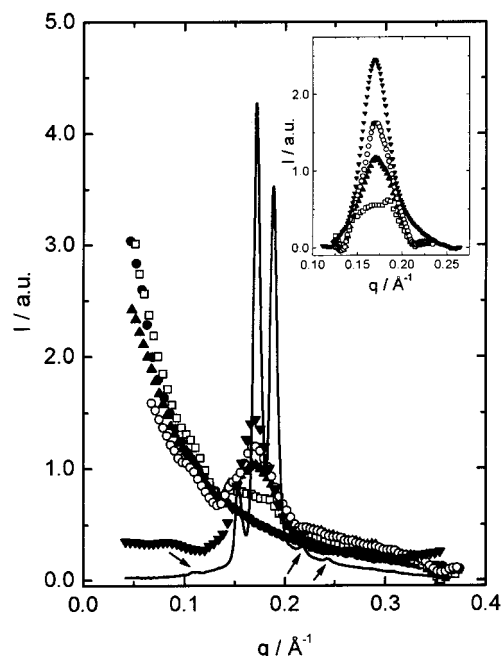


Figure 5. SAXS patterns for pure 0.47% NaPA (●) and for NaPA/DPC complexes with increasing S/P ratios in water: S/P = 0.3 (□), 0.5 (▲), 0.7 (○), 0.9 (▼), and 1.5 (solid curve). The arrows are pointing to the weak scattering peaks. In the inset, the scattering in the region of the interference maximum, after subtracting the background, is shown for solutions with S/P = 0.3, 0.5, 0.7, and 0.9.

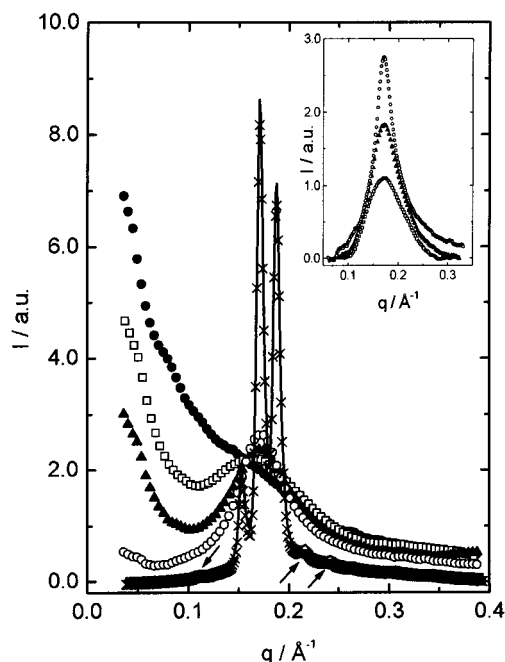


Figure 6. SAXS patterns for pure 0.54% NaPMA (●) and for NaPMA/DPC complexes with increasing S/P ratios in water: S/P = 0.3 (□), 0.6 (▲), 0.8 (○), 1.0 (×), and 1.5 (solid curve). The arrows are pointing to the weak scattering peaks. In the inset, the scattering in the region of the interference maximum, after subtracting the background, is shown for solutions with S/P = 0.3, 0.6, and 0.8.

q -values (larger \bar{a} -values), that is, to $q_m = 0.172$ and 0.175 \AA^{-1} in the presence of NaPA and NaPMA, respectively. Careful analysis of the shape of the main maximum makes clear that underlying structures are more complex (cf. inset in Figure 4). The main observed maximum could be the result of the overlap of two to three peaks. By now,

Table 2. Structural Parameters of NaPA/DPC and NaPMA/DPC Complexes in Water Obtained from the Peak(s) in the SAXS Curves

system	S/P	$q_m/\text{\AA}^{-1}$	$\bar{a}/\text{\AA}$	$\beta_s \times 10^2/\text{rad}$	$L/\text{\AA}$	$r_m/\text{\AA}$	Δ/\bar{a}
NaPA/DPC	0.3	0.172	36.6	1.23	106	168	0.19
	0.5	0.172	36.5	0.924	141	223	0.16
	0.7	0.172	36.5	0.616	183	289	0.14
	0.9	0.170	36.9	0.605	205	323	0.13 ₅
	1.5 (peak 1)	~0.109	57.6				
	1.5 (peak 2)	0.154	40.7				
	1.5 (peak 3)	0.172	36.5				
	1.5 (peak 4)	0.188	33.3				
	1.5 (peak 5)	~0.217	29.0				
	1.5 (peak 6)	~0.242	26.0				
NaPMA/DPC	0.3	0.175	36.0	1.41	88	139	0.20
	0.6	0.175	35.9	1.19	104	165	0.19
	0.8	0.174	36.1	0.97	128	261	0.17
	1.0 (peak 1)	0.154	40.8				
	1.0 (peak 2)	0.171	36.6				
	1.0 (peak 3)	0.189	33.5				
	1.0 (peak 4)	~0.217	28.9				
	1.0 (peak 5)	~0.242	26.0				
	1.5 (peak 1)	~0.109	57.6				
	1.5 (peak 2)	0.154	40.8				
	1.5 (peak 3)	0.171	36.6				
	1.5 (peak 4)	0.189	33.5				
	1.5 (peak 5)	~0.216	29.0				
	1.5 (peak 6)	~0.242	26.0				

however, there is no evidence for this and a more extensive study on the quantitative level is in progress. With increasing surfactant content, the intensity of the peak increases; however, its position remains almost unchanged. Therefore, the \bar{a} -spacing is around 36.5 and 36.0 Å in NaPA/DPC and NaPMA/DPC complexes, respectively, for all the S/P ratios investigated. The structural parameters for these samples are given in Table 2. The L and r_m values increase, whereas Δ/\bar{a} decreases with increasing S/P. The Δ/\bar{a} values are lower than 0.2, indicating a more ordered system than in the NaPSS/DPC case.

3. DPC + NaPA or NaPMA: $S/P \geq 1.0$. Solutions with S/P close to or higher than 1 contain pieces of a sticky complex in a turbid solution. The latter shows a similar scattering pattern to that observed for samples with $S/P \leq 0.7$ (see above); however, the scattering intensity is considerably lower in this case. This implies that the surfactant-polyelectrolyte aggregate is still present in the solution but in a rather small amount. On the other hand, the diffraction pattern of the precipitate displays a much more ordered structure. As one can see in Figures 5 and 6, three sharp peaks appear in the q -range where one peak has been observed for lower surfactant content. Careful analysis of the solid curves in Figures 5 and 6 (for $S/P = 1.5$) reveals additional peaks at q -values around 0.109, 0.217, and 0.242 Å⁻¹. The positions of all the peaks are given in Table 2 in q -values and in corresponding \bar{a} -values. One can see that the peaks are very sharp (β_s is low). Consequently, the Δ/\bar{a} value becomes very small and parameters L and r_m increase substantially. It has been stated before that one cannot encounter extremely low values of Δ/\bar{a} (high values of L and r_m) in a real system; therefore, these values are not given in Table 1 for $S/P = 1.0$ and 1.5. The $\sin^2 \theta$ values for each diffraction peak are in the ratio 2:4:5:6:8:10, which indicates that they can be attributed to the reflection from (110), (200), (210), (211), (220), and (310) planes of the cubic lattice of a space group $Pm\bar{3}n$.^{34,41f} The lattice constants for the NaPA/DPC and NaPMA/DPC complexes are equal to 81.6 and 81.9 Å, respectively. This corresponds roughly to 2.5 diameters

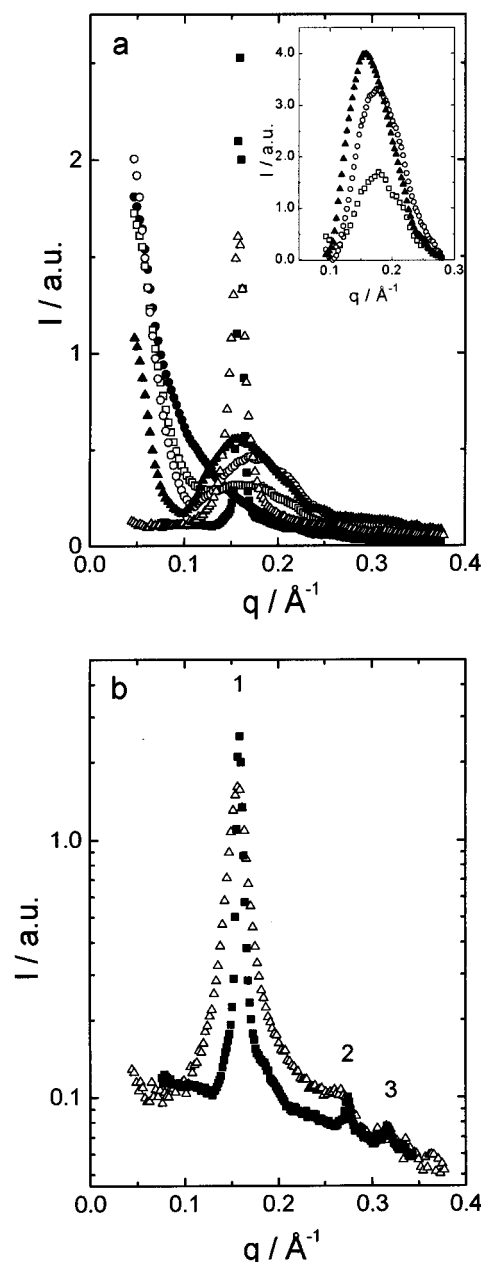


Figure 7. (a) SAXS patterns for pure 1% NaPSS (●) and for NaPSS/CPC complexes with increasing S/P ratios in water: S/P = 0.3 (□), 0.5 (○), 0.7 (▲), 1.0 (△), and 1.3 (■). In the inset, the scattering in the region of the interference maximum, after subtracting the background, is shown for solutions with S/P = 0.3, 0.5, and 0.7. (b) SAXS pattern for the stoichiometric NaPSS/CPC complex (S/P = 1.0 and 1.3, symbols are the same as in part a). The peaks are designated by numbers 1, 2, and 3 (cf. Table 1).

of a globular DPC micelle. A similar cell parameter is found for DTAB incorporated in a cross-linked NaPA network.¹⁵

B. Solutions with CPC. 1. CPC + NaPSS: $S/P < 1.0$. The behavior of NaPSS/CPC solutions in this S/P range is very similar to the NaPSS/DPC case (cf. Figure 7a). The scattering peak is found in the q -range from about 0.178 to 0.165 Å⁻¹. As in the case of complexes between NaPSS and DPC, the peak is shifted to lower q -values and its relative intensity increases with increasing S/P. All the structural parameters for NaPSS/CPC solutions are reported in Table 1. The values of \bar{a} increase from 35.2 to 38 Å for S/P = 0.3 and 0.7, respectively. The L , r_m , and Δ/\bar{a} values are fairly constant as observed before for

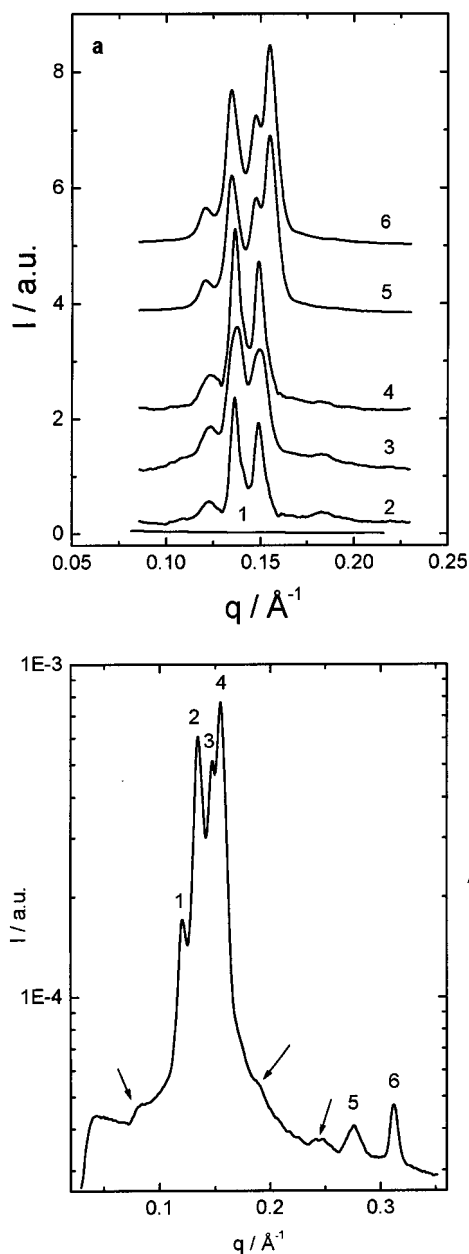


Figure 8. (a) SAXS patterns for pure 0.47% NaPA (curve 1) and for NaPA/CPC complexes in water (curves 2–6, corresponding to $S/P = 0.3, 0.5, 0.7, 1.0,$ and 1.5 , respectively). For clarity, the patterns are displaced by an appropriate integer. (b) SAXS pattern for NaPA/CPC complex with $S/P = 1.5$. The numbers 1–6 designate the main peaks (for positions, see Table 3). The arrows are pointing to the weak scattering peaks, which are not included in the numbering.

NaPSS/DPC solutions. Their slightly higher values point to a more ordered arrangement between the PSS anion and the surfactant with a longer hydrocarbon chain.

2. CPC + NaPSS: $S/P \geq 1.0$. The scattering curves obtained for the NaPSS/CPC complex at $S/P = 1.0$ and 1.3 are shown in Figure 7b. They exhibit an intense main peak accompanied by two well-resolved higher order peaks. A smooth scattering curve with no peak was observed in the equilibrium solution. This is a solution of free (unbound) surfactant; its concentration is below 0.5% (no peak is detected in the scattering curve for the detergent concentrations below 5%). The q_m -values and the corresponding \bar{a} -spacing values for the peaks of the NaPSS/CPC complex are given in Table 1. Because of low β_S values (sharp peaks!), the L and r_m values increase more than

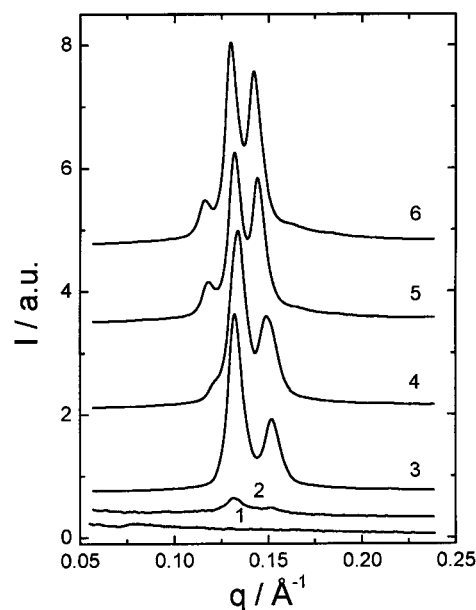


Figure 9. SAXS patterns for pure 0.54% NaPMA (curve 1) and for NaPMA/CPC complexes in water (curves 2–6, corresponding to $S/P = 0.3, 0.6, 0.8, 1.0,$ and 1.5 , respectively). The X-ray intensity of NaPMA/CPC with $S/P = 0.3$ is multiplied by a factor of 5. For clarity, the patterns are displaced by an appropriate integer.

10 times in comparison with the values found in NaPSS/CPC solutions with $S/P \leq 0.7$. Consequently, the degree of disorder is considerably smaller than 0.1. For the same reason as stated above, L , r_m , and Δ/\bar{a} are not reported. Instead, the $\sin^2 \theta$ values for each diffraction peak are evaluated. They correspond to the sequence 1:3:4 (or in q_m -values to the sequence 1:1.72:2) and indicate a hexagonal close-packed arrangement of surfactant in the complexes.³⁴ The calculated unit cell dimension is equal to 39.5 Å. According to Tanford's formula³⁵ for the length of a fully extended hexadecyl (C_{16}) chain, the radius of a globular CPC micelle is equal to 20.5 Å. Therefore, the above dimension corresponds approximately to one diameter of a CPC micelle.

3. CPC + NaPA ($S/P < 1$) and CPC + NaPMA. Scattering curves in NaPA/CPC and in NaPMA/CPC solutions are shown in Figures 8 and 9. It is observed that the intensity of the scattered radiation in pure polyelectrolyte solutions is considerably lower than in solutions mixed with surfactant. Consequently, no background correction was necessary in these cases. The most striking feature of the patterns in Figures 8a and 9 is the existence of two (NaPMA/CPC with $S/P = 0.3$) to three very sharp peaks in the q -region from about 0.12 to 0.15 Å⁻¹. The peaks change neither their position nor their relative intensity upon changing the S/P ratio. One recalls that a similar scattering pattern was found for complexes of these two polyelectrolytes with DPC, however only for S/P ratios above 1.0, whereas with CPC the highly ordered structures are detected already at the lowest S/P value studied. The positions of all the peaks in q_m -values and in the corresponding \bar{a} -spacing values are given in Table 3. The $\sin^2 \theta$ values for each diffraction peak fit to the sequence 4:5:6 (or in q_m -values to $\sqrt{4}:\sqrt{5}:\sqrt{6}$). A similar structure was observed in pure 20% CPC at 10 °C, in NaPA(NaPMA)/DPC complexes with $S/P \geq 1$ (see above), and also for other systems reported in the literature.^{15,16} The lattice constants for the NaPA/CPC and NaPMA/CPC complexes were calculated to be 102.5 and 107 Å, respectively. As in the case of complexes between NaPA or NaPMA and DPC,

Table 3. Position of Maxima and Characteristic \bar{a} -Spacings Obtained from the SAXS Patterns for NaPA/CPC and NaPMA/CPC Complexes in Water

system	S/P	$q_m/\text{\AA}^{-1}$						$\bar{a}/\text{\AA}$					
		1 max	2 max	3 max	4 max	5 max	6 max	1 max	2 max	3 max	4 max	5 max	6 max
NaPA/CPC	0.3	0.123	0.137	0.149				51.2	46.0	42.1			
	0.5	0.123	0.137	0.149				51.0	45.9	42.0			
	0.7	0.123	0.137	0.149				51.0	45.9	42.0			
	1.0	0.122	0.135	0.148	0.155	0.275	0.312	51.4	46.5	42.4	40.5	22.8	20.1
	1.5	0.122	0.135	0.148	0.155	0.256	0.296	51.4	46.5	42.4	40.5	24.5	21.2
NaPMA/CPC	0.3		0.132	0.150					47.5	41.8			
	0.6		0.133	0.151		0.258			47.4	41.8		24.3	
	0.8		0.134	0.149		0.259			46.9	42.1		24.3	
	1.0	0.119	0.133	0.144		0.238	0.270	53.0	47.4	43.6		26.4	23.3
	1.5	0.117	0.131	0.142				53.8	48.1	44.2			

this corresponds approximately to 2.5 diameters of a globular CPC micelle.

4. *CPC + NaPA (S/P ≥ 1)*. For the NaPA/CPC complexes with S/P = 1.0 and 1.5, an additional very intense peak is observed at $q_m = 0.155 \text{ \AA}^{-1}$ and several rather weak peaks (indicated by the arrows in Figure 8b) are found at around 0.085, 0.19, and 0.24 \AA^{-1} . The latter three together with peaks 1, 2, and 3 (see Table 3) correspond to a $\sin^2 \theta$ sequence equal to 2:4:5:6:10:16 and point to a similar cubic structure as found in NaPA(NaPMA)/DPC complexes with S/P ≥ 1 .

In all these scattering patterns, the relative location 1 could not be seen. A similar finding was reported previously for the cubic phase in pure surfactant/water systems⁴¹ and for the one formed by cetyltrimethylammonium acetate in the presence of NaPA.^{13b} It was argued in the second case^{13b} that the first diffraction order is presumably too weak or too close to the beam center to be observed. It could be that the presence of the polyelectrolyte chains contributes to the extinction or to the lowering of the intensity of some peaks. Besides the relative location 1, the relative location 8 is also not seen in Figure 8b. From the results obtained for NaPA/DPC complexes, one would expect this peak to be present. Obviously, the very intense peak 4 obscures the latter one in the NaPA/CPC case.

In addition to the above ones, two well-pronounced peaks at q_m -values of 0.275 and 0.312 \AA^{-1} can be seen. Together with peak 4, they correspond to a $\sin^2 \theta$ sequence of 1:3:4. This type of diffraction pattern is characteristic for a hexagonal arrangement and was observed before for the stoichiometric complexes between NaPSS and CPC (compare Figures 7b and 8b).

To summarize, in the cases of NaPA/CPC complexes with S/P ≥ 1 , one observes two coexisting ordered structures, a cubic one and a hexagonal one, which is superimposed on the diffraction pattern of the first one. The lattice constant for the hexagonal phase in the NaPA/CPC system is equal to 40.5 Å.

Discussion

The scattering results suggest that different ordered structures appear in the investigated polyelectrolyte-surfactant complex solutions. They depend on the nature of the polyion, on the surfactant hydrocarbon chain length, and also on the S/P ratio. Table 4 summarizes various surfactant organizations in complexes. In the first part, structures for which one more or less broad peak is found in the scattering curves are discussed. Afterward, examples of multiple and higher order peaks are examined. Whenever appropriate, the scattering patterns in polyelectrolyte/surfactant mixed systems will be compared with the ones in pure surfactant solutions.

Table 4. Various Phases Found in the Anionic Polyelectrolyte-Cationic Surfactant Systems

surfactant		polyelectrolyte		
		NaPA	NaPMA	NaPSS
DPC	S/P < 1	micellar	micellar	micellar
	S/P ≥ 1	cubic	cubic	micellar
CPC	S/P < 1	cubic	cubic	micellar
	S/P ≥ 1	cubic + hexagonal	cubic	hexagonal

I. Complexes with One Broad Peak. 1. *NaPSS/DPC (all S/P) and NaPSS/CPC (S/P ≤ 0.7)*. The maximum in NaPSS/DPC and NaPSS/CPC solutions appears at considerably lower q -values than in pure surfactant solutions. In fact, at surfactant concentrations comparable to those of the surfactant in mixed solutions with the polyelectrolyte, no maximum is found (compare Figures 1 and 2 with Figures 4 and 7a, respectively). This finding implies that the distance between surfactant aggregates in the complexes is considerably shorter than the distance between surfactant micelles in the polymer-free solutions. The reported \bar{a} -spacing is the center-to-center distance between the micelles consecutively bound to the polyion. One can conclude that the polyelectrolyte chain forces the micelles together.

The characteristic size \bar{a} in the NaPSS/surfactant system is from 5.2 to 2.6 Å and from 5.8 to 3 Å shorter than twice the length of an extended C₁₂ or C₁₆ hydrocarbon chain, respectively.³⁵ These results suggest that DPC and CPC bind to the PSS anion in the form of micelles, which are smaller in size than micelles formed in pure detergent solutions. This observation can be explained by the specific interaction that can take place between the polyion-induced surfactant micelle and the PSS chain. It was found by NMR measurements² that the aromatic benzene-sulfonate rings on the PSS anion solubilize in the hydrocarbon-like interior of the surfactant aggregate. Irrespective of the size of the surfactant tail, a typical aggregate with the PSS chain can be visualized as a complex where several micelles are surrounded by the polyion charges in such a way that some of the aromatic rings are embedded in the micelle surface. This could lead to smaller micellar aggregates. A more appropriate term for these surfactant micelles would be mixed micelles, whereas the whole formation of several micelles connected with the polyion chain could be called an aggregate-of-aggregates.

The \bar{a} -spacing in NaPSS/surfactant solutions increases with increasing S/P ratio, whereas the ordering parameters are rather constant up to S/P = 0.7. This can be explained by the growth of micelles bound to the polyion, that is, by the increase of their aggregation number, whereas the number of micellelike aggregates per polymer chain remains nearly constant. The small decrease in Δ/\bar{a} for S/P = 0.9 and 1.5 could be a consequence of the

coalescence of complex aggregates when their net charge is decreased.

2. *NaPA/DPC and NaPMA/DPC ($S/P < 1$)*. In these solutions, the value of \bar{a} is approximately constant (cf. Table 2) and exceeds the length of two C_{12} chains by about 5 Å. It corresponds approximately to the size of the surfactant micelle together with a layer of the polyion chain that is wrapped around it (the radii of the PA and PMA anions are in the range from 5.5 to 6 Å). The ionic side groups on the PA and PMA chains are hydrophilic COO^- groups that have no tendency to incorporate in the hydrocarbon-like interior of the surfactant micelle as was the case with the aromatic groups attached to the PSS chain.³⁶ Therefore, the flexible PA and PMA anions simply form loops around surfactant aggregates. They compensate the charge of the micelles and cause an electrostatic attraction between them. One is prompted to believe that the aggregates with NaPA or NaPMA are rather loose in comparison with the ones with NaPSS.

It has been found by fluorescence measurements³⁷ that the aggregation number of the PA-induced micelle of DTAB is rather insensitive to the S/P ratio; it is approximately the same as in pure DTAB solutions above the cmc. Therefore, the NaPA- and NaPMA-induced surfactant micelles resemble very closely the ordinary micelles in size. When more and more surfactant is added to the solution of the PA (or PMA) anion, the number of micelles increases but their size remains constant. This is supported by the observed constant increase in parameters L and r_m (or a constant decrease in Δ/\bar{a}) with increasing S/P ratio in this and in our previous studies.³⁸ It is worthwhile stressing that the used polyelectrolyte concentration is 100 times higher than the concentration usually applied for binding studies or fluorescence measurements.^{9,20–22,37} Therefore, the average distances between the polyions are shorter and the aggregated surfactant could play a role of “cross-links” in a networklike organization of the polyelectrolyte chains.

Finally, we have to point out the differences in ordering parameters obtained in the presence of the two polyelectrolytes with hydrophilic functional groups. On the average, L and r_m are lower (Δ/\bar{a} is higher) in NaPMA/DPC than in NaPA/DPC solutions. This suggests that the association of surfactant with the PA chain is stronger than with the PMA chain, which is in accordance with the literature.³⁹ In dilute solutions, the degree of binding of surfactants to the PMA anion is somewhat lower than the corresponding value obtained for the PA anion. Consequently, the ordered regions in the complexes with PMA are smaller for the same S/P ratio.

II. Complexes with Several Sharp Peaks. 1. NaPSS/CPC ($S/P \geq 1$). As observed before for the NaPSS/DPC complex, an essential increase in ordering is found in the NaPSS/CPC complex when the equimolar S/P ratio is approached or exceeded. Moreover, a crystalline-like structure develops in the NaPSS/CPC precipitate in which the surfactant is arranged in a hexagonal close-packed lattice. One is not surprised by this observation, taking into account the well-known fact that polyelectrolyte-surfactant interactions increase with increasing the length of the nonpolar surfactant chain. The degree of binding of CPC to NaPSS is almost 100% (compare with the value

of 80% for DPC),^{4,9} implying that every charged group on the polyanion is blocked by surfactant cations. Therefore, the charge of the chain (or, vice versa, of the micelle) is completely compensated leading to the mutual flocculation of the uncharged NaPSS/CPC aggregates. This leads to the occurrence of a very compact hexagonal phase in equilibrium with a dilute solution of free surfactant.

In fact, any phase sufficiently concentrated in surfactant is expected to be ordered. To see if one also encounters a hexagonal arrangement in pure CPC solutions, scattering experiments in a 20% solution of this surfactant have been performed. Nevertheless, the scattering pattern of the solution at 25 °C revealed no crystalline-like organization (Figure 3). To “condense” the CPC solution still further, the solution was cooled below its Krafft point (around 11 °C for CPC in water⁴⁰). At 10 °C, a crystalline-like structure developed (solid curve in Figure 3). For comparison, the total CPC concentration in the NaPSS/CPC solution with $S/P = 1.3$ is around 6%; nevertheless, a hexagonal phase is observed. Again, we recall that the specific interaction between the PSS chain and the surfactant micelle is responsible for this. A similar hexagonal structure has been reported recently for the arrangement of sodium dodecyl sulfate in the chemically cross-linked gels of poly-(diallyltrimethylammonium chloride).^{17,18} A gel state may present a similar restriction for the spatial distribution of the surfactant as the polystyrenesulfonate chain.

2. *NaPA/CPC (S/P below 1) and NaPMA/CPC (all S/P)*. The structure in NaPA (NaPMA)/CPC complexes displays a considerably more ordered situation than in pure CPC solutions at 10 °C or in complexes with DPC. A cubic arrangement (NaPA/CPC for $S/P < 1$ and NaPMA/CPC for all S/P) is followed by a coexistence of a cubic and a hexagonal structure (NaPA/CPC for $S/P \geq 1$). Repeatedly, the interaction of CPC is somewhat weaker with NaPMA than with NaPA. This can be concluded from the fact that fewer peaks were observed in NaPMA/CPC complexes than in NaPA/CPC ones (cf. Table 3). There is an indication of the development of a hexagonal structure in the NaPMA/CPC case, but it cannot be unequivocally confirmed because the intense first peak of a hexagonal phase is absent in this case.

The unit cell dimension of the cubic phase is larger in CPC aggregates in the presence of NaPA (NaPMA) than in pure 20% CPC solutions at 10 °C. It corresponds approximately to a sum of two micellar³³ and two polyion-chain diameters (see results section). This structure could correspond to a simple cubic lattice,^{15,16} formed by eight more or less spherical micelles that are encircled by the polyelectrolyte chain.

It has been mentioned¹³ that there is a tendency of micelle-aggregates to grow into a rodlike shape at sufficiently high surfactant concentrations. A schematic picture of the structure of the hexagonal phase made by the addition of NaPA to a dilute micellar solution of CTAB has been recently proposed by Ilekci et al.¹³ (see Figure 5 in ref 13b). The CTAB and CPC surfactants have the same size of the nonpolar part of the molecule. Therefore, one may believe that the structure is largely the same in both cases; that is, the surfactant is arranged in long cylinders that are connected with the polyion chain into a tightly packed hexagonal mesophase. One of the reasons that a similar arrangement could not be observed in pure CPC is its limited solubility at room temperature. A hexagonal phase is usually not formed until the surfactant concentration reaches around 60%.⁴¹

(36) Kogej, K.; Škerjanc, J. *Acta Chim. Slov.* **1999**, *46* (4), 481.

(37) Hansson, P.; Almgren, M. *J. Phys. Chem.* **1995**, *99*, 16684.

(38) Kogej, K.; Evmenenko, G.; Theunissen, E.; Škerjanc, J.; Berghmans, H.; Reynaers, H.; Bras, W. *Macromol. Rapid Commun.* **2000**, *21*, 1226.

(39) Kiefer, J. J.; Somasundaran, P.; Ananthapadmanabhan, K. P. *Langmuir* **1993**, *9*, 1187.

(40) Heckmann, K.; Schwarz, R.; Strnad, J. *J. Colloid Interface Sci.* **1987**, *120*, 114.

One can conclude that a large cluster of polyelectrolyte–surfactant aggregates is formed in NaPA/CPC and NaPMA/CPC mixed solutions. In some parts of this cluster, the surfactant micelles still remain discrete and are arranged in a cubic lattice, but in other parts the micelles grow into a rodlike or even cylindrical shape. This enables a more compact packing of the aggregates and results in a hexagonal structure. It is very likely that the transition from globular to cylindrical CPC micelles in complexes is continuous. On the other hand, the electrostatic repulsion between micelles in pure surfactant solutions prevents a more close-packed arrangement. In the presence of a polyelectrolyte, this repulsion is effectively screened by the polyion charges and this can finally lead to a “flocculation” of the aggregates.

Similar crystalline-like organization of surfactant is reported for the aggregates of DPC in a charged polymer network of poly[2-(acrylamido)-2-methylpropanesulfonic acid].¹⁶ At an S/P ratio equal to 0.79, in the latter case suddenly three peaks appeared, being consistent with the primitive cubic lattice. For $S/P \leq 0.67$, no clear peak has been detected. Hansson¹⁵ studied self-assembly of DPC in the slightly cross-linked gel of NaPA and found that no evident peaks could be observed for $S/P \leq 0.75$. Once again, at higher surfactant content several narrow peaks appeared, pointing to various space groups of a cubic structure. It has to be stressed that the cubic structure in NaPA/CPC and NaPMA/CPC complexes in our case emerges already at lower S/P ratios than in the above examples and, what is especially important, in solutions of linear nongelling polyelectrolytes. This again confirms that CPC has a stronger tendency to form ordered structures than its shorter hydrocarbon chain counterpart, DPC.

Conclusions

Mixed solutions of alkylpyridinium surfactants and polyvinyl-based polyelectrolytes display different types of organizations. The surfactant is arranged in micellelike aggregates, but the formation of higher order structures depends on the characteristics of the polyelectrolyte chain. In particular, the PSS chain distinguishes itself from the other two, that is, from PA and PMA. The NaPSS-induced

micelle appears to be from 2.6 to 5.8 Å smaller in size than a free one. This could be a consequence of a lower aggregation number of surfactant in the aggregate and of the inclusion of hydrophobic aromatic groups of the PSS chain into the micelle. By our opinion, the situation in complexes with PSS is the closest to the “pearl-necklace” picture proposed for polymer–surfactant aggregates.^{1c} When the charge of the PSS ion is completely neutralized by the surfactant (this only takes place with the longer-chain surfactant, CPC), a hexagonal close-packed structure develops. In the concentration and temperature ranges applied in this study, no hexagonal phase was found in pure CPC solutions. It is obvious that the PSS anion effectively “concentrates” the surfactant.

In complexes with the hydrophilic PA and PMA chains, the polyelectrolyte-induced micelles recollect the ordinary ones in size. Polyion chains play a role of a counterion cloud, and by making loops around the surface of charged surfactant micelles they connect them into a cubiclike structure followed by a coexistence of a cubic and a hexagonal phase (NaPA/CPC) at an approximately equimolar ratio of charged groups of the surfactant and the polyelectrolyte. One could propose that the surfactant micelles play a role of entanglement sites for the polymer. Contrary to the aggregates with PSS, where one chain is associated with several micelles, one micelle in the PA or PMA complexes could connect several chains. This could lead to a networklike organization between PA(PMA) and surfactant. A cubic arrangement of micelles is indicated also in pure CPC solutions; however, in the complexes it is observed at considerably lower CPC concentrations.

The ordering is more pronounced in complexes with DPC than in the ones with CPC. In fact, DPC induces crystalline-like structure only with the hydrophilic chains (PA and PMA) when the 1:1 surfactant to polyelectrolyte ratio is reached or exceeded.

Acknowledgment. This work was supported by the Flemish Institute for Science and Technology (IWT), the Fund for Scientific Research-Flanders (FWO), INTAS (96-1115) and the Belgian Government (IUAP-IV/11). The authors are indebted to the staff of the DUBBLE team at the ESRF, Grenoble, for their experimental support. Professor L. Piculles is thanked for his helpful discussions prior to the preparation of the manuscript. K.K. is grateful to H.B. and H.R. for enabling her stay at KULeuven. H.R. and E.T. thank FWO-Flanders for a research grant. G.E. is a fellow researcher of the “Bijzonder Onderzoeksfonds KULeuven”.

LA001249X

(41) (a) Balmбра, R. R.; Clunie, J. S.; Goodman, J. F. *Nature* **1969**, *222*, 1159. (b) Luzzati, V.; Reiss-Husson, F. *Nature* **1966**, *210*, 1351. (c) Luzzati, V.; Tardieu, A.; Gulik-Krzywicki, T.; Rivas, E.; Reiss-Husson, F. *Nature* **1968**, *220*, 485. (d) Auvray, X.; Petipas, C.; Anthorne, R. *J. Phys. Chem.* **1989**, *93*, 7458–7464. (e) McGrath, K. M. *Langmuir*, **1995**, *11*, 1835. (f) Sakya, P.; Seddon, J. M.; Templer, R. H.; Mirkin, R. J.; Tiddy, G. J. T. *Langmuir* **1997**, *13*, 3706.